Research Square

Preprints are preliminary reports that have not undergone peer review.
They should not be considered conclusive, used to inform clinical practice,
or referenced by the media as validated information.

Integrating Binary Silva Classification and Tumor Size for Predicting Survival in Early-Stage HPV-Associated Endocervical Adenocarcinoma

Linman Wang
Affiliated Hospital of Guizhou Medical University
Fenghu Li
Affiliated Hospital of Guizhou Medical University
Zhenglin Li
Guizhou Medical University
Xue Tian
Affiliated Hospital of Guizhou Medical University
Fan Mei
Affiliated Hospital of Guizhou Medical University
Lili Hu
Affiliated Hospital of Guizhou Medical University
Yanjun Du
Affiliated Hospital of Guizhou Medical University
Yidan Gong
Guizhou Medical University
Jiehui Li
ljiehui123@163.com

Affiliated Hospital of Guizhou Medical University

Research Article

Keywords: HPV-associated endocervical adenocarcinoma, Binary Silva pattern, Predictive model, Lymphovascular space invasion, Risk stratification

Posted Date: November 16th, 2026

DOI: https://doi.org/10.21203/rs.3.rs-11450518/v1

License: This work is licensed under a Creative Commons Attribution 4.0 International License.
Read Full License

Additional Declarations: No competing interests reported.

Integrating Binary Silva Classification and Tumor Size for Predicting Survival in Early-Stage HPV-Associated Endocervical Adenocarcinoma

Linman Wang[1,2,3], Fenghu Li[1,2,3], Zhenglin Li[2], Xue Tian[1,2,3], Fan Mei[1,3], Lili Hu[1,2,3], Yanjun Du[1,2,3], Yidan Gong[2], Jiehui Li[1,2,3*]

[1]Department of Oncology, Affiliated Hospital of Guizhou Medical University, Guiyang, Guizhou 550004, China
[2]Department of Oncology, Guizhou Medical University, Guiyang, Guizhou 550004, China
[3]Department of Oncology, Guizhou Medical University Affiliated Cancer Hospital, Guizhou 550004, China

Correspondence:
Jiehui Li, MD, Department of Oncology, Affiliated Hospital of Guizhou Medical University, Guiyang 550004, Guizhou, China; Email: ljiehui123@163.com

Abstract

Background: The optimal risk stratification for early-stage human papillomavirus-associated endocervical adenocarcinoma (HPVA) lacking conventional major high-risk factors remains clinically challenging. This study aimed to evaluate the independent prognostic utility of the binary Silva classification in this specific population and to develop a validated progression-free survival (PFS) nomogram for individualized risk assessment.

Methods: We retrospectively evaluated 163 patients with FIGO 2018 stage IA2–IIA2 HPVA who underwent radical surgery and lacked major high-risk pathological factors (e.g., lymph node metastasis). Patients were categorized into low- and high-risk binary Silva groups based on morphological invasive patterns and lymphovascular space invasion (LVSI) status. Multivariable Cox proportional hazards regression was utilized to identify independent prognosticators. A predictive PFS nomogram was constructed and internally validated utilizing 1,000 patient-level bootstrap resamples to calculate optimism-corrected performance metrics.

Results: Over a median follow-up of 48 months (95% CI, 40–59), the high-risk binary Silva group (n=82) exhibited significantly inferior PFS and overall survival compared with the low-risk group (n=81; P<0.001 and P=0.0015, respectively). Multivariable analysis confirmed that high-risk binary Silva status (hazard ratio [HR], 4.37; 95% CI, 1.64 – 11.62; P=0.003) and tumor size ≥2 cm (HR, 4.05; 95% CI, 1.57 – 10.42; P=0.004) were robust independent adverse predictors for PFS. The resulting two-factor predictive nomogram demonstrated favorable internal validity, yielding an optimism-corrected concordance index (C-index) of 0.717.

Conclusion: The binary Silva classification serves as a powerful, independent prognostic stratifier for early-stage HPVA without major high-risk factors. By integrating binary Silva status with tumor size, our internally validated nomogram provides a quantitative, practical framework to refine postoperative risk assessment and potentially guide individualized adjuvant treatment strategies.

Keywords: HPV-associated endocervical adenocarcinoma; Binary Silva pattern; Predictive model; Lymphovascular space invasion; Risk stratification

1 Introduction

Cervical cancer remains one of the most prevalent gynecological malignancies worldwide[1-3]. While systematic screening programs have successfully driven a global decline in cervical squamous cell carcinoma, the relative proportion of endocervical adenocarcinoma (EAC) continues to escalate[4, 5]. Biologically and clinically distinct from squamous cell carcinoma, early-stage EAC exhibits unique recurrence trajectories[6, 7]. However, current clinical management paradigms and risk stratification frameworks remain disproportionately reliant on legacy cohorts dominated by squamous histology, which inherently fail to capture the prognostic distinctiveness of the EAC population.

Recognizing this etiological and morphological heterogeneity, the 2020 World Health Organization (WHO) classification and the International Endocervical Adenocarcinoma Criteria and Classification (IECC) formally integrated human papillomavirus (HPV) status as a core diagnostic criterion, isolating HPV-associated endocervical adenocarcinoma (HPVA)[8, 9]. To further refine prognostication within HPVA, the morphologically driven Silva classification was introduced. Recently, to mitigate inter-observer variability and enhance clinical pragmatism, a binary Silva framework was proposed, effectively stratifying patients into low-risk (Patterns A and B without lymphovascular space invasion [LVSI]) and high-risk (Pattern B with LVSI, and Pattern C) categories[10, 11]. Emerging spatial transcriptomic analyses have provided preliminary biological validation for this two-tiered morphological divergence[12].

Despite these pathological advancements, the clinical translatability of the binary Silva classification for guiding adjuvant therapy remains unverified in critical subgroups. A recent international multicenter study led by the ISGyP confirmed the binary system's predictive superiority; however, their findings were confounded by the inclusion of patients harboring major high-risk pathological factors, such as nodal metastasis[11]. Concurrently, adjuvant treatment decisions for early-stage disease still default to the Sedlis criteria (evaluating tumor size, LVSI, and stromal invasion depth)[13]. The extrapolation of these criteria to EAC is highly controversial, as the prognostic weight of LVSI and recurrence patterns in early-stage EAC fundamentally differ from squamous disease[14]. Consequently, for patients with early-stage HPVA who lack major high-risk factors but harbor LVSI or high-risk Silva patterns, current guidelines offer no definitive therapeutic consensus[15].

To bridge this critical evidence gap, this retrospective cohort study focuses exclusively on patients with early-stage HPVA devoid of major high-risk pathological factors. Our primary objective was to rigorously evaluate the independent prognostic value of the binary Silva classification within this specific population. Secondarily, we sought to develop and internally validate a quantitative progression-free survival (PFS) nomogram integrating binary Silva status with tumor size. By translating morphological risk into a tangible predictive tool, this study aims to provide objective evidence for individualized postoperative risk assessment, ultimately informing future strategies to optimize adjuvant treatment intensity.

2 Materials and methods

2.1 Study population

This retrospective cohort study evaluated patients diagnosed with HPVA who underwent radical hysterectomy with pelvic lymphadenectomy at two affiliated hospitals of Guizhou Medical University between June 2013 and June 2024. The study protocol was approved by the Institutional Review Board of the Guizhou Medical University Affiliated Cancer Hospital (Approval No.: SL-202606170), with a waiver of informed consent granted due to the retrospective design. From an initial screening of 180 longitudinal visit records, duplicate follow-up entries for the same individuals (n=17) were merged and resolved, yielding a final analytical cohort of 163 unique patients.

2.2 Inclusion and exclusion criteria

Eligibility criteria mandated: (1) patient age ≥ 18 years; (2) postoperative histological confirmation of HPVA, classified according to the IECC and the 2020 WHO standards[16] ; (3) International Federation of Gynecology and Obstetrics (FIGO) 2018 stage IA2 to IIA2 disease; and (4) the definitive absence of major high-risk pathological factors, strictly defined as negative surgical margins, negative pelvic lymph nodes, and no parametrial invasion. Exclusion criteria comprised tumors of unknown origin, metastatic cervical cancer, unclassifiable Silva invasion patterns, and the presence of concurrent life-threatening comorbidities.

2.3 Pathological classification and grouping

To systematically evaluate prognostic variations driven by morphological invasion and LVSI, patients were stratified using three progressive classification frameworks. Initially, the traditional three-tier system categorized tumors into Pattern A, Pattern B, and Pattern C[17-19] (Figure 1). A four-tier expansion subsequently subdivided Pattern B by LVSI status (Pattern A, Pattern B [LVSI−], Pattern B [LVSI+], and Pattern C). Ultimately, the focal binary Silva classification dichotomized the cohort into a low-risk group (Pattern A and Pattern B [LVSI−]) and a high-risk group (Pattern B [LVSI+] and Pattern C)[20-22]. Tumor size was categorically defined as <2 cm or ≥2 cm, reflecting established clinical guideline thresholds rather than post-hoc data optimization.

2.4 Follow-up

Longitudinal clinical follow-up was maintained via outpatient clinic surveillance and telephone interviews, with follow-up time calculated from the date of primary surgery. The primary clinical endpoint was PFS, defined as the interval from surgery to the first documented disease progression or death from any cause. Overall survival (OS) served as a secondary exploratory endpoint, measured from surgery to death. For cases involving consolidated duplicate records, the earliest documented event date was applied for endpoint analysis, whereas the latest confirmed progression-free or survival date was utilized for right-censoring.

2.5 Statistical analysis

Data processing was performed using SPSS Statistics, and statistical analyses were conducted in R (version 4.5.2) using the survival package. Continuous variables were compared using Welch's t-test and categorical variables using Pearson's chi-square or Fisher's exact test, as appropriate. Missing data were summarized by variable (Supplementary Table S1). Kaplan–Meier curves and log-rank tests were used to compare PFS and OS across the three-tier, four-tier, and binary Silva classifications; analyses used patients with an available value for the relevant classification (Supplementary Figure S1). The primary multivariable PFS Cox model included 162 patients with 26 events after exclusion of one patient with missing tumor size. Hazard ratios (HRs) and 95% confidence intervals (CIs) were estimated using the Efron method for tied events. The proportional hazards assumption was assessed using Schoenfeld residual tests and plots for the primary PFS and exploratory OS models (Supplementary Figures S5 and S6; Supplementary Table S4). For prediction model development and comparison, a common complete-case cohort of 161 patients with 25 PFS events was used, additionally excluding one patient without a classifiable traditional three-tier Silva pattern. The binary two-factor model included tumor size and binary Silva status; the comparator models included tumor size with traditional three-tier Silva status, or tumor size alone. Internal validation used 1,000 patient-level bootstrap resamples. Performance measures included Harrell's C-index, inverse probability of censoring weighted (IPCW) cumulative/dynamic AUC, and IPCW Brier scores. Apparent time-dependent ROC curves at 3 and 5 years were distinguished from optimism-corrected performance estimates (Supplementary Figure S2). Paired differences in apparent discrimination between the binary and traditional two-factor models were summarized with bootstrap percentile intervals (Supplementary Figure S3). Apparent calibration was assessed using Kaplan–Meier observed event risks for the four predictor profiles. Exploratory IPCW decision curve analysis with internal optimism correction compared model-guided strategies with the treat-all and treat-none reference strategies at 3 and 5 years across thresholds of 1%–50% (Supplementary Figure S4). Subgroup HRs and interaction tests were examined where estimable (Supplementary Figure S7); sparse or structurally absent comparison groups limited these exploratory analyses.

3 Results

3.1 Baseline patient characteristics

The analytical cohort comprised 163 unique HPVA patients, stratified by the binary Silva framework into low-risk (n = 81) and high-risk (n = 82) groups. Baseline demographics and baseline tumor parameters, including age (P = 0.627), tumor size (P = 0.113), and differentiation grade (P = 0.141), were well-balanced between the cohorts. In contrast, the high-risk cohort was significantly enriched with advanced FIGO stages (P = 0.004), deeper stromal invasion ($\geqslant$1/3, P = 0.023), and perineural invasion (P = 0.002). By definition, LVSI was exclusively present in the high-risk group (50.0%). The distribution of postoperative adjuvant therapies also varied significantly (P < 0.001). Missing covariate data were explicitly tabulated (Table 1; e.g., age missing in 9

cases, tumor grade in 16 cases, stromal depth in 3 cases) to ensure analytical transparency.

3.2 Survival analysis

Median follow-up estimated by the reverse Kaplan–Meier method was 48 months (95% CI, 40–59). PFS and OS differed across both the traditional three-tier classification (log-rank P=0.003 and P<0.001, respectively) and the four-tier classification (P=0.005 and P=0.001, respectively; Supplementary Figure S1). The three-tier analysis included 162 patients with available classification (Pattern A, n=29; Pattern B, n=69; Pattern C, n=64), whereas the four-tier and binary analyses included all 163 patients. The four-tier groups comprised Pattern A (n=29), Pattern B without LVSI (n=52), Pattern B with LVSI (n=18), and Pattern C (n=64). These curves describe prognostic separation and do not, by themselves, establish the superiority of one classification scheme over another. In the binary analysis, PFS events occurred in 5 of 81 low-risk patients and 21 of 82 high-risk patients. The high-risk group had poorer PFS (log-rank P<0.001) and exploratory OS (P=0.0015; Figure 2). At 60 months, estimated PFS was 94.4% (95% CI, 82.4%–98.3%) in the low-risk group and 74.3% (95% CI, 61.2%–83.6%) in the high-risk group, with 32 and 25 patients remaining at risk, respectively. Time-specific survival estimates are provided in Supplementary Table S2.

3.3 Univariate and multivariate analyses

Univariable Cox results are presented in Supplementary Table S3. In the primary multivariable PFS model (n=162, 26 events), tumor size ≥2 cm (HR, 4.05; 95% CI, 1.57–10.42; P=0.004) and high-risk binary Silva status (HR, 4.37; 95% CI, 1.64–11.62; P=0.003) were associated with poorer PFS after mutual adjustment (Table 2). Schoenfeld residual tests did not detect a departure from proportional hazards for tumor size (P=0.413), binary Silva status (P=0.422), or the global primary PFS model (P=0.518; Supplementary Figure S5; the primary_full model in Supplementary Table S4). These diagnostics do not establish that proportional hazards holds at every follow-up time. In the sensitivity analysis excluding two patients with conflicting longitudinal endpoint records (n=160, 24 events), the associations persisted for tumor size ≥2 cm (HR, 4.43; 95% CI, 1.60–12.28; P=0.004) and binary high-risk status (HR, 4.05; 95% CI, 1.51–10.89; P=0.006; Supplementary Table S5). In the exploratory OS model (n=161, 12 deaths), the HR was 2.85 for tumor size ≥2 cm (95% CI, 0.76–10.75; P=0.122) and 12.37 for high-risk binary Silva status (95% CI, 1.59–96.21; P=0.016; Supplementary Table S8). However, the global proportional hazards test indicated a departure from the assumption (P=0.0368), accompanied by time variation in the residual diagnostic plots (Supplementary Figure S6; Supplementary Table S4). Together with the small number of deaths and wide CIs, this limits interpretation of the OS HRs as constant effects over follow-up.

3.4 Nomogram construction and validation

The exploratory two-factor nomogram was developed in the common prediction cohort of 161 patients with 25 PFS events to estimate 3- and 5-year PFS (Figure 3). The

apparent Harrell's C-index was 0.728 (bootstrap percentile interval, 0.662–0.830), and the optimism-corrected C-index was 0.717. The optimism-corrected IPCW AUCs at 3 and 5 years were 0.761 and 0.787, respectively, and the corrected calibration slope was 0.925 (Table 3). Supplementary Figure S2 displays the apparent cumulative/dynamic ROC curves for the binary two-factor, traditional two-factor, and tumor-size-only models. The apparent 3- and 5-year AUCs were 0.767 and 0.797 for the binary model and 0.780 and 0.817 for the traditional model. These curves were evaluated in the development cohort and should not be interpreted as externally validated or optimism-corrected ROC curves. Paired comparisons of apparent discrimination between the binary and traditional two-factor models are shown in Supplementary Figure S3. The differences (binary minus traditional) were −0.004 for the C-index (95% percentile interval, −0.041 to 0.066), −0.013 for the 3-year AUC (−0.046 to 0.067), and −0.020 for the 5-year AUC (−0.067 to 0.038; Supplementary Table S7). All intervals included zero, so these analyses did not establish superiority of the binary model. Equivalence was not evaluated using a prespecified margin. Apparent calibration for the four actual predictor profiles is shown in Figure 4 and remains subject to development-sample optimism and substantial uncertainty in sparse profiles. The exploratory optimism-corrected decision curves at 3 and 5 years are presented in Supplementary Figure S4. The binary model showed positive estimated net benefit over part of the examined threshold range, but this was not sustained across the full 1%–50% range. The curves for competing models crossed, indicating that the relative net benefit depended on the selected threshold. These analyses therefore provide an exploratory assessment under the decision-curve assumptions; they do not establish a validated treatment threshold, demonstrate a causal benefit from adjuvant therapy, or support uniform clinical superiority of the binary model.

3.5 Stratified analysis and interaction effects

Exploratory subgroup HRs for high-risk versus low-risk binary Silva status are shown in Supplementary Figure S7. Point estimates were above 1 in the estimable strata, but several CIs were wide and crossed 1. No statistically significant interaction was detected for age (P=0.473), FIGO stage (P=0.551), or postoperative adjuvant modality (P=0.464). These nonsignificant tests do not establish a homogeneous prognostic association or comparable treatment effects across subgroups. In patients with tumors <2 cm, no PFS event occurred in the low-risk group (0/40), compared with six events in the high-risk group (6/30), precluding a reliable finite ordinary Cox subgroup estimate. The LVSI-positive stratum contained no binary low-risk patients, whereas the shallow stromal-invasion stratum had no event in the low-risk group. These non-estimable contrasts reflect sparse events or the group definition and should not be interpreted as evidence of absent risk. Accordingly, the tumor-size-stratified findings were interpreted descriptively and not as evidence of effect modification.

4 Discussion

In this retrospective cohort of patients with early-stage HPVA without major high-risk pathological factors, high-risk binary Silva classification and tumor size ⩾2 cm were

associated with poorer PFS after mutual adjustment (HR = 4.37 and 4.05, respectively). A two-factor nomogram incorporating these variables achieved an optimism-corrected C-index of 0.717 following internal bootstrap validation. These findings suggest that binary Silva classification may contribute to postoperative prognostic assessment in this population, although the model requires external validation before clinical implementation.

Our findings robustly extend recent international collaborative efforts. While the traditional three-tier Silva classification revolutionized HPVA prognostication, it remained plagued by inter-observer variability, particularly in distinguishing Pattern A from Pattern B lacking LVSI[10, 23]. The ISGyP recently advocated for the binary framework to streamline this process and improve risk prediction[10, 11]. However, their landmark study included patients with node-positive disease—a potent overriding risk factor[11, 24]. Our study uniquely advances this paradigm by confirming that even in a strictly node-negative, early-stage cohort, the binary framework maintains profound prognostic fidelity. Furthermore, our clinical survival data align seamlessly with recent spatial transcriptomic analyses[20], which identified distinct molecular architectures underpinning these high-risk invasion patterns, providing a biological rationale for the accelerated recurrence trajectories observed in our high-risk cohort.

The clinical imperative of our nomogram becomes evident when navigating adjuvant therapeutic decisions, which are currently tethered to the legacy Sedlis criteria[25, 26]. Originally derived from squamous cell cohorts, the Sedlis criteria prioritize LVSI, tumor size, and stromal depth[25, 27]. Intriguingly, in our multivariable models, traditional LVSI status and FIGO staging lost statistical independence when competing against binary Silva status. This phenomenon does not biologically negate LVSI—which by definition is inextricably integrated into the high-risk binary category—but rather suggests that the binary morphological pattern encapsulates and mathematically supersedes isolated traditional risk factors in early-stage HPVA. Therefore, applying unmodified squamous-centric guidelines to EAC may obscure true risk profiles, underscoring the clinical utility of our histology-specific nomogram.

The interpretation of our nomogram must be contextualized within its methodological framework. A major strength is the stringent selection criteria, actively excluding major high-risk factors (e.g., positive margins, parametrial involvement) to isolate a clinically ambiguous population. However, several critical limitations remain. First, the strictly early-stage nature of the cohort intrinsically restricted the event volume (26 PFS events), which, compounded by missing baseline covariates, limited the statistical precision of our hazard estimates. Second, OS analyses violated the proportional hazards assumption, relegating those findings to hypothesis generation. Crucially, while the model selection process was mathematically exploratory, our bootstrap validation provided unique insights: during 1,000 resamples, the traditional three-tier model triggered 362 non-convergence warnings due to data sparsity, whereas the binary model triggered only 14. This stark contrast highlights the superior statistical stability and practical applicability of the binary framework in limited-sample, low-event scenarios, yet simultaneously underscores the inherent fragility of modeling rare events.

5 Conclusion

In this retrospective cohort of patients with early-stage HPVA without major high-risk pathological factors, high-risk binary Silva classification was associated with poorer PFS after adjustment for tumor size. An exploratory nomogram incorporating these two variables showed potential for postoperative risk assessment following internal validation, but superiority over the traditional three-tier Silva model was not established. Given the limited number of events, potential treatment-related confounding, and absence of external validation, these findings do not support changes to adjuvant treatment based on the model. External validation in larger, independent cohorts is required before clinical implementation.

Declarations

Author Contributions

All authors contributed to the study conception and design. The first draft of the manuscript was written by Linman Wang and Zhenglin Li, and all authors commented on previous versions of the manuscript. Conceptualization, methodology, and overall project administration were performed by Jiehui Li and Fenghu Li. Material preparation, data curation, and clinical follow-up were conducted by Zhenglin Li, Xue Tian, Lili Hu, Yanjun Du, and Yidan Gong. Formal data analysis and statistical interpretation were executed by Fan Mei and Xue Tian. All authors read, critically revised, and approved the final submitted version of the manuscript, and agreed to be accountable for all aspects of the work.

Funding

This study was supported by the Science and Technology Department of Guizhou Province (Grant No. Qiankehe Chengguo LC[2026] General 312).

Institutional Review Board Statement

The study was conducted in accordance with the Declaration of Helsinki and approved by the Ethics Committee of Guizhou Medical University Affiliated Cancer Hospital (Approval No.: SL-202606170).

Informed Consent Statement

Patient consent was waived by the reviewing Institutional Review Board due to the retrospective nature of the study, which utilized anonymized clinical data.

Data Availability Statement

The datasets generated and analyzed during the current study are not publicly available to safeguard patient privacy but are available from the corresponding author on reasonable request, subject to institutional ethical policies.

Conflicts of Interest

The authors declare that they have no competing interests relevant to this work.

Acknowledgments

We would like to express our profound gratitude to all the patients, clinicians, and nursing staff at the participating institutions for their contributions to this study.

References

1. An S, Han A, Lin Z, Quan H: **Targeting ferroptosis in cervical cancer: Mechanistic insights and therapeutic opportunities**. *Cell Signal* 2025, **136**:112122.
2. Lu L, Wang F, Wang T, Xing Z, Jiang P: **Hypoxia drives cervical cancer progression via OCT4/ORAI3-dependent glycolysis and Ca(2+) signaling**. *Cell Mol Life Sci* 2025, **82**(1):390.
3. Zhang Y, Li C, Xiang Y: **Tumor immune microenvironment in cervical cancer: Histological subtype-specific immune landscapes and therapeutic implications**. *Biochim Biophys Acta Rev Cancer* 2026, **1881**(3):189581.
4. Bray F, Laversanne M, Sung H, Ferlay J, Siegel RL, Soerjomataram I, Jemal A: **Global cancer statistics 2022: GLOBOCAN estimates of incidence and mortality worldwide for 36 cancers in 185 countries**. *CA: a cancer journal for clinicians* 2024, **74**(3):229-263.
5. Li S, Liu C, Weng L: **Exploring Cervical Adenocarcinoma: Epidemiological Insights, Diagnostic and Therapeutic Challenges, and Pathogenetic Mechanisms**. *Cancer medicine* 2025, **14**(2):e70620.
6. Yao G, Qiu J, Zhu F, Wang X: **Survival of Patients With Cervical Cancer Treated With Definitive Radiotherapy or Concurrent Chemoradiotherapy According to Histological Subtype: A Systematic Review and Meta-Analysis**. 2022, **9**:843262.
7. Yüksel D, Çakır C, Kılıç F, Ünsal M, Kılıç Ç, Kimyon Cömert G, Korkmaz V, Türkmen O, Turan T: **Oncologic outcomes of patients with FIGO 2014 stage IB-IIA cervical adenocarcinoma who underwent radical surgery**. *Archives of gynecology and obstetrics* 2022, **306**(5):1657-1664.
8. Stolnicu S: **Role of human papillomavirus status in the classification, diagnosis, and prognosis of malignant cervical epithelial tumors and precursor lesions**. *Pathologie (Heidelberg, Germany)* 2026, **47**(Suppl 1):97-103.
9. Stolnicu S, Barsan I, Hoang L, Patel P, Terinte C, Pesci A, Aviel-Ronen S, Kiyokawa T, Alvarado-Cabrero I, Pike MC *et al*: **International Endocervical Adenocarcinoma Criteria and Classification (IECC): A New Pathogenetic Classification for Invasive Adenocarcinomas of the Endocervix**. *The American journal of surgical pathology* 2018, **42**(2):214-226.
10. Zyla RE, Dodington DW, Pakbaz S, Terzic T, Robinson C, Clarke B, Rouzbahman M, Hodgson A: **Assessment of Interobserver Agreement Among Gynecologic Pathologists Between Three-Tier Versus Binary Pattern-based Classification Systems for HPV-associated Endocervical Adenocarcinoma**. *The American journal of surgical pathology* 2024, **48**(12):1522-1529.
11. Powell A, Hodgson A, Cohen PA, Rabban JT, Park KJ, McCluggage WG, Gilks CB, Singh N, Oliva E: **Improved Risk Prediction in Human Papillomavirus-Associated Endocervical Adenocarcinoma Through Assessment of Binary Silva Pattern-based Classification: An International Multicenter Retrospective Observational Study Led by the International Society of Gynecological Pathologists (ISGyP)**. *International journal of gynecological pathology : official journal of the International Society of Gynecological Pathologists* 2024, **43**(5):436-446.
12. Axelrod ML, Zhou R, Sun L: **Spatial transcriptomic landscape of invasion patterns in human**

papillomavirus-associated endocervical adenocarcinoma. *Scientific reports* 2026, **16**(1):13246.

13. Sedlis A, Bundy BN, Rotman MZ, Lentz SS, Muderspach LI, Zaino RJ: **A randomized trial of pelvic radiation therapy versus no further therapy in selected patients with stage IB carcinoma of the cervix after radical hysterectomy and pelvic lymphadenectomy: A Gynecologic Oncology Group Study**. *Gynecologic oncology* 1999, **73**(2):177-183.
14. Bae BK, Bae H, Cho WK, Kim BG, Choi CH, Kim TJ, Lee YY, Lee JW, Kim HS, Park W: **Risk Factors Affecting Clinical Outcomes of Low-risk Early-stage Human Papillomavirus-Associated Endocervical Adenocarcinoma Treated by Surgery Alone: Application of Silva Pattern**. *International journal of gynecological pathology : official journal of the International Society of Gynecological Pathologists* 2024, **43**(5):447-456.
15. Wang X, Xu J, Zhang H, Qu P: **Integrating the Silva pattern into clinical practice: a prognostic tool for tailoring surgery and adjuvant therapy in cervical adenocarcinoma**. *Cancer treatment and research communications* 2026, **47**:101187.
16. Cree IA, White VA, Indave BI, Lokuhetty D: **Revising the WHO classification: female genital tract tumours**. *Histopathology* 2020, **76**(1):151-156.
17. Chen M, Han L, Wang Y, Chen Y, Zheng A: **Association between Silva pattern-based classification and endocervical adenocarcinoma: a systematic review and meta-analysis**. *Int J Gynecol Cancer* 2024, **34**(11):1704-1710.
18. Zyla RE, Dodington DW, Pakbaz S, Terzic T, Robinson C, Clarke B, Rouzbahman M, Hodgson A: **Assessment of Interobserver Agreement Among Gynecologic Pathologists Between Three-Tier Versus Binary Pattern-based Classification Systems for HPV-associated Endocervical Adenocarcinoma**. *Am J Surg Pathol* 2024, **48**(12):1522-1529.
19. Felicelli C, Smith SH, Griffin B, Grubs A, Strom D, Shanes E, Strickland A, Purdy J, Novo JE, Wei J-J *et al*: **The Silva pattern-based classification for HPV-associated endocervical adenocarcinoma: A single institution concordance study of trainees and gynecologic pathologists**. *Pathol Res Pract* 2024, **257**:155311.
20. Axelrod ML, Zhou R, Sun L: **Spatial transcriptomic landscape of invasion patterns in human papillomavirus-associated endocervical adenocarcinoma**. *Sci Rep* 2026, **16**(1).
21. Matsubara M, Otani T, Kawakami F, Koike A, Hirayama T, Yamanishi Y, Horikawa N, Emoto I, Ukita M, Sumitomo M *et al*: **Cervical adenocarcinoma risk stratification using histotype and invasion pattern: a multicenter retrospective study by the KAMOGAWA Study Group**. *Gynecol Oncol* 2025, **200**:112-121.
22. Hagen KK, Lie AK, Dahl GF, Eyjolfsdottir B, Wang Y, Ranum P, Skilbrei M, Lund KV, Sugulle M, Staff AC *et al*: **The Silva pattern-based classification and oncological outcomes in women undergoing fertility-sparing surgery for early-stage cervical cancer**. *Int J Gynecol Cancer* 2025, **35**(9):102012.
23. Felicelli C, Smith SH, Griffin B, Grubs A, Strom D, Shanes E, Strickland A, Purdy J, Novo JE, Wei JJ *et al*: **The Silva pattern-based classification for HPV-associated endocervical adenocarcinoma: A single institution concordance study of trainees and gynecologic pathologists**. *Pathol Res Pract* 2024, **257**:155311.
24. Wei LJ, Wu ZY, Wu LY, Wu YW, Liang HY, Luo RZ, Liu LL: **Prognostic implications of immune classification based on PD-L1 expression and tumor-infiltrating lymphocytes in endocervical adenocarcinoma**. *Transl Oncol* 2025, **52**:102265.

25. Restaino S, Pellecchia G, Arcieri M, Bogani G, Taliento C, Greco P, Driul L, Chiantera V, Ercoli A, Fanfani F *et al*: **Management for Cervical Cancer Patients: A Comparison of the Guidelines from the International Scientific Societies (ESGO-NCCN-ASCO-AIOM-FIGO-BGCS-SEOM-ESMO-JSGO)**. *Cancers (Basel)* 2024, **16**(14).
26. Petousis S, Almperis A, Margioula-Siarkou C, Guyon F, Pergialiotis V, Thomakos N, Dinas K, Rodolakis A: **Adjuvant Treatment for Surgically-Treated Cervical Cancer Patients: A Comprehensive Review**. *Cancers (Basel)* 2025, **17**(22).
27. Wang Z, Chu R, Wu N, Yuan M, Song X, Tian W, Yang C, Wan J, Wang G: **Development and validation of prognostic prediction models for early-stage cervical cancer patients based on pathological intermediate-risk factors**. *Ther Adv Med Oncol* 2025, **17**:17588359251359461.

Table 1. Baseline clinicopathological characteristics stratified by the binary Silva classification (n=163)

Variables	Low-risk group (n=81)	High-risk group (n=82)	P-value
Age (years), mean (SD)	46.77 (9.49)	47.49 (9.03)	0.627*
Tumor size, n (%)			0.113
<2 cm	40 (49.4%)	30 (37.0%)	
≥2 cm	41 (50.6%)	51 (63.0%)	
Missing	0	1	
FIGO stage, n (%)			0.004
I	74 (91.4%)	61 (74.4%)	
II	7 (8.6%)	21 (25.6%)	
Perineural invasion, n (%)			0.002
Absent	79 (97.5%)	68 (82.9%)	
Present	2 (2.5%)	14 (17.1%)	
LVSI, n (%)			< 0.001
Absent	81 (100.0%)	41 (50.0%)	
Present	0 (0.0%)	41 (50.0%)	
Tumor differentiation, n (%)			0.141
G1	12 (15.8%)	4 (5.6%)	
G2	52 (68.4%)	54 (76.1%)	
G3	12 (15.8%)	13 (18.3%)	
Missing	5	11	
Depth of stromal invasion, n (%)			0.023
<1/3	21 (26.6%)	10 (12.3%)	
≥1/3	58 (73.4%)	71 (87.7%)	

Missing	2	1	
Postoperative adjuvant therapy, n (%)			< 0.001
Radiotherapy	62 (77.5%)	34 (42.5%)	
Chemoradiotherapy	18 (22.5%)	46 (57.5%)	
Missing	1	2	

Note: Data are presented as counts and percentages. Percentages were calculated utilizing valid (non-missing) denominators to ensure analytical transparency. P-values were derived from Welch's t-test for continuous variables, and Pearson's chi-square test or Fisher's exact test for categorical variables.

Table 2. Multivariable Cox proportional hazards regression for predictors of progression-free survival (n=162)

Variables	Hazard Ratio (HR)	95% Confidence Interval (CI)	P-value
Tumor size			
<2 cm	Reference		
≥2 cm	4.05	1.57–10.42	0.004
Binary Silva classification			
Low risk	Reference		
High risk	4.37	1.64–11.62	0.003

Note: The multivariable analysis was performed on the primary survival cohort (n=162, 26 events), following the exclusion of one patient with missing tumor size data. Abbreviations: PFS, progression-free survival; HR, hazard ratio; CI, confidence interval.

Table 3. Internal validation and discriminative performance of the two-factor predictive models (n=161)

Metric	Binary Two-Factor Model		Traditional Two-Factor Model	
	Apparent	Optimism-corrected	Apparent	Optimism-corrected
Harrell C-index	0.728	0.717	0.732	0.714
3-year IPCW AUC	0.767	0.761	0.780	0.770
5-year IPCW AUC	0.797	0.787	0.817	0.805
3-year IPCW Brier score	0.104	0.110	0.107	0.113
Calibration slope	1.000	0.925	1.000	0.645

Note: Model performance was evaluated in the complete-case prediction cohort. Internal validation metrics were optimism-corrected utilizing 1,000 patient-level bootstrap resamples. The apparent concordance index (C-index) difference between the binary and traditional Silva models was −0.004 (paired bootstrap percentile interval: −0.041 to 0.066). Abbreviations: C-index, concordance index; IPCW, inverse probability of censoring weighted.

Figure 1. Morphological features of the traditional three-tier Silva classification. Representative hematoxylin and eosin (H&E)-stained sections illustrating Silva Pattern A (a), Pattern B (b), and Pattern C (c). Scale bars = 1000 μm.

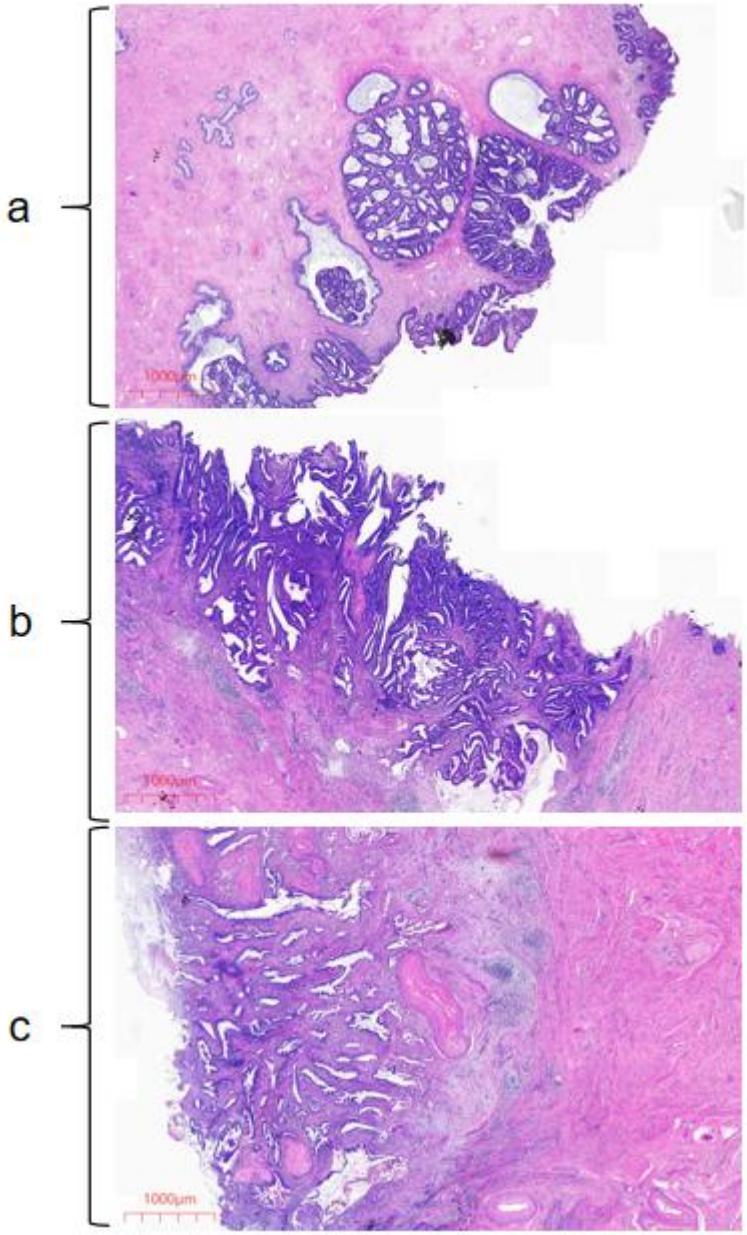


Figure 2. Survival outcomes stratified by the binary Silva classification.
Kaplan–Meier survival curves for PFS (left) and exploratory OS (right) in the entire cohort (n=163). Tick marks indicate censored events. The numbers of patients at risk at specified time points are tabulated below each panel. P-values were calculated utilizing two-sided log-rank tests.

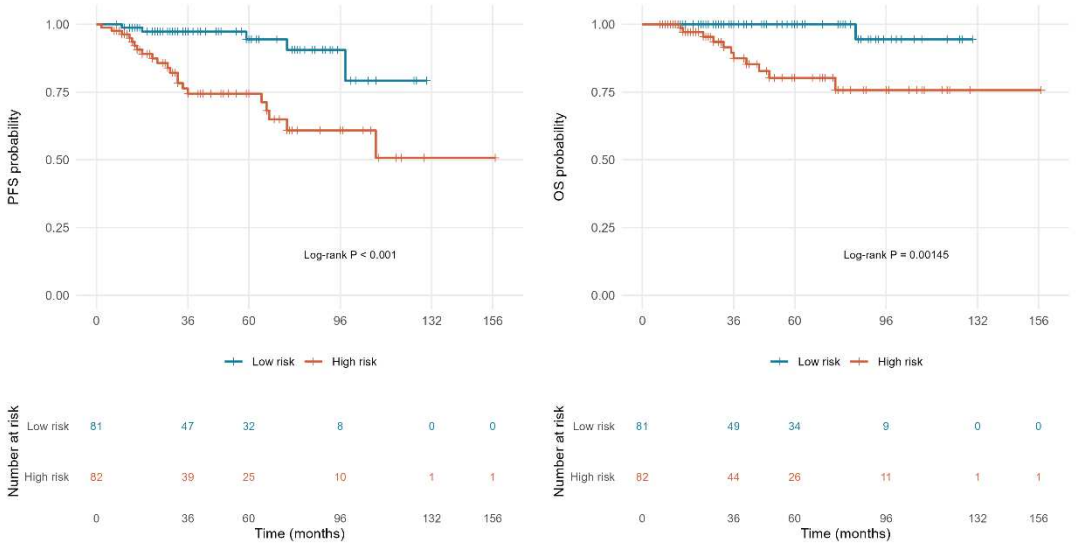


Figure 3. Predictive nomogram for PFS in early-stage HPV-associated endocervical adenocarcinoma.

The two-factor nomogram integrates binary Silva classification and tumor size to quantify 3-year and 5-year PFS probabilities. The model was developed and evaluated in the common prediction cohort (n=161, 25 events).

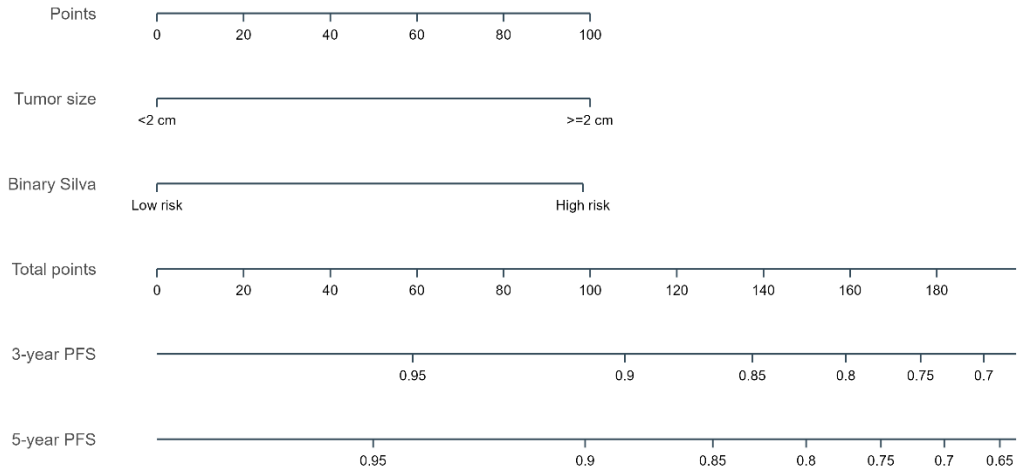
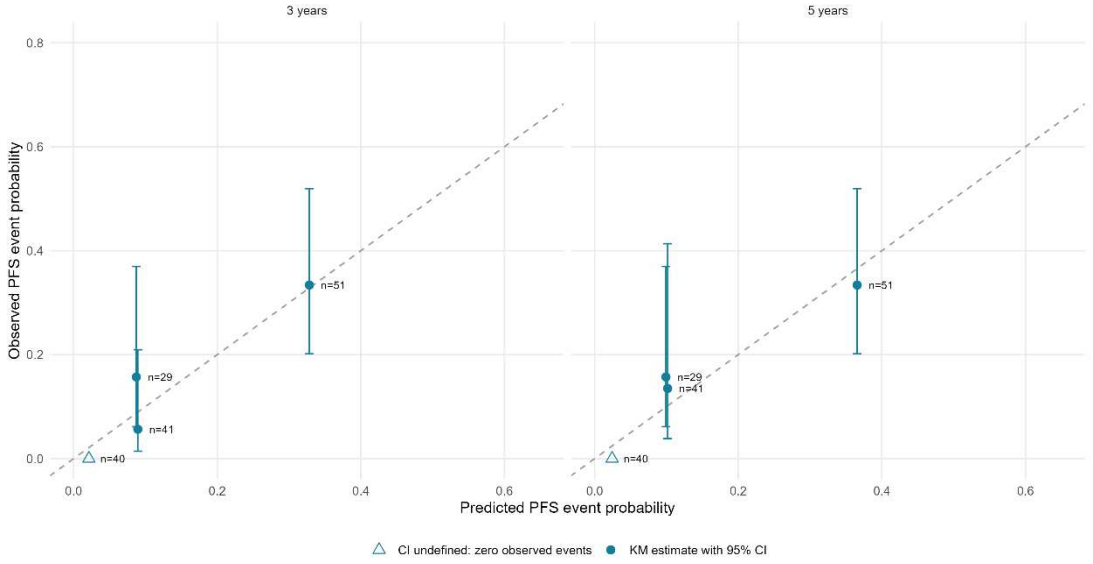


Figure 4. Apparent calibration plots for the two-factor PFS nomogram.
Calibration performance is assessed at 3 years (left) and 5 years (right) in the prediction cohort (n=161). The dashed diagonal line represents ideal perfect prediction. Solid points denote the four actual predictor profiles, with associated labels indicating sample sizes. Observed event probabilities were estimated via Kaplan–Meier analysis, and error bars depict 95% CI where estimable.



Supplementary Files

This is a list of supplementary files associated with this preprint. Click to download.

- SupplementaryMaterials.docx